CONF-9004138--4

DE90 010581

TREAT REACTOR CONTROL ROD SCRAM SYSTEM SIMULATIONS AND TESTING

by

C. W. Solbrig and W. W. Stevens

Argonne National Laboratory
Reactor Experiments and Examinations Division
Box 2528
Idaho Falls, Idaho 83403

Abstract

Air cylinders moving heavy components (100 to 300 lbs) at high speeds (above 300 in/sec) present a formidable end-cushion-shock problem. With no speed control, the moving components can reach over 600 in/sec if the air cylinder has a 5 ft stroke.

This paper presents an overview of a successful upgrade modification to an existing reactor control rod drive design using a computer model to simulate the modified system performance for system design analysis. This design uses a high speed air cylinder to rapidly insert control rods (278 lb moved 5 ft in less than 300 msec) to scram an air-cooled test reactor. Included is information about the computer models developed to simulate high-speed air cylinder operation and a unique new speed control and end cushion design. A patent application is pending with the U.S. Patent & Trade Mark Office for this system (DOE case number S-68,622). The evolution of the design, from computer simulations thru operational testing in a test stand (simulating in-reactor operating conditions) to installation and use in the reactor, is also described.

1. INTRODUCTION

The Transient Reactor Test Facility (TREAT) completed a major reactor systems modification in January 1990, its first since initial criticality in 1959. TREAT is an air cooled test reactor designed to evaluate reactor fuels and structural materials under conditions simulating various types of nuclear excursions. It is located near Idaho Falls, Idaho, USA, and is operated for the United States Department of Energy by Argonne National Laboratory.

The reactor has eight shutdown-control rod drives which position 12 control rods. Four drives position dual control rods and four position single control rods. Both types of rod drives use a vertically mounted high-pressure air cylinder with a 60 inch stroke. Each air cylinder piston rod is mechanically connected to the control rod(s). The TREAT rod drives are located underneath the reactor, and when the control rods are fully down (the air cylinder piston at its lowest position) the reactor is in a shutdown mode (see Figure 1).

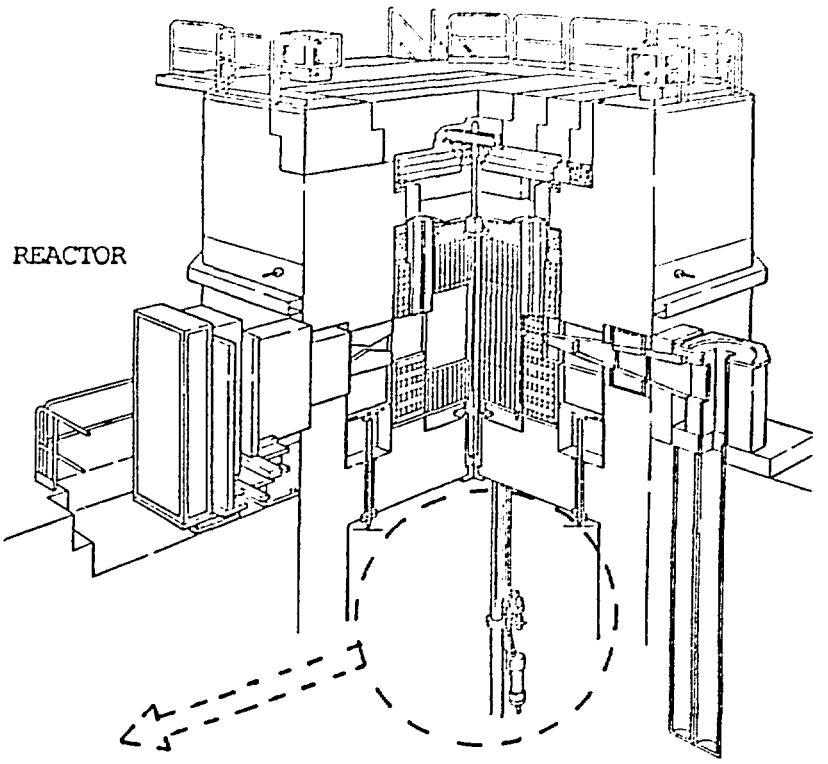

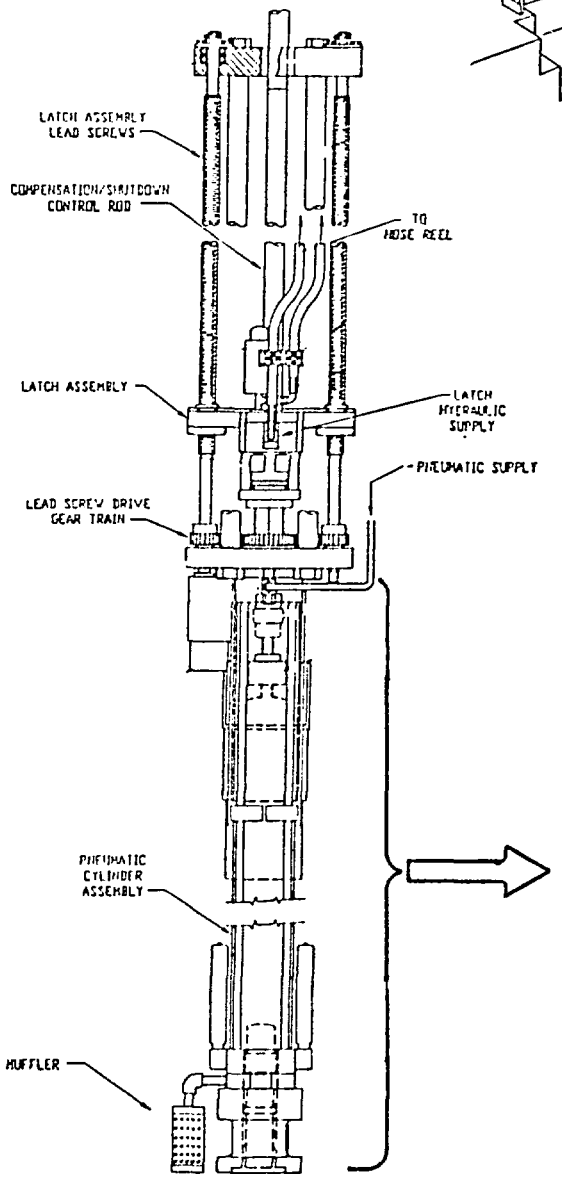

Control Rod Drive Assembly
(Single Control Rod Type)

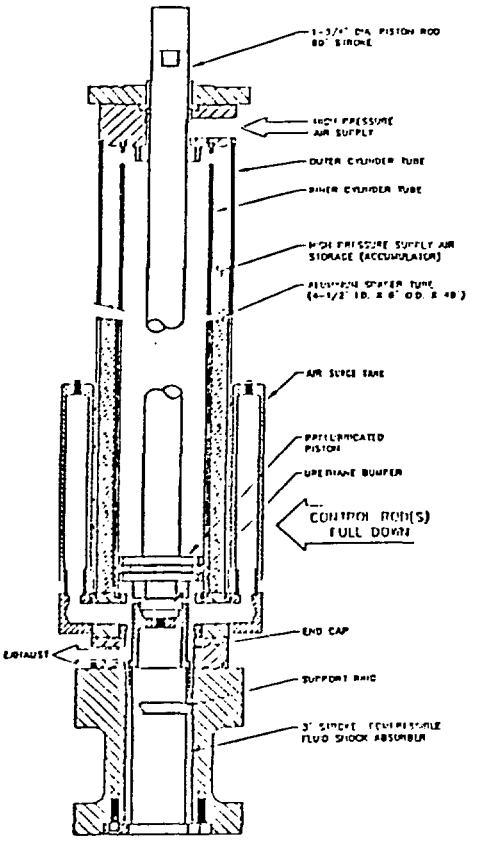

Air Cylinder Assembly
(Typical)

Fig. 1 TREAT Reactor and Control Rod Drive Section Views

The control rods are attached to the drives by an extension rod. When the drive piston is raised, the extension rod pushes the poison section out of the core. The maximum drive travel of 60 inches moves the poison section from full in to full out of the 48 inch tall core. Control of the reactor reactivity during steady-state operation is achieved by fine vertical adjustment of the control rods through the use of an electrically driven lead-screw elevating mechanism on each control rod drive.

The air cylinder piston rod (and control rod(s)) are moved by a lead-screw mechanism for reactor operation. Operating the lead-screw in the up direction mechanically elevates the piston rod against the downward force of the high-pressure air on the upper side of the air cylinder piston. As the air cylinder piston is lifted air pressure is controlled by a back pressure relief valve in the rod drive scram air supply system. To scram the reactor, a rapid-release (40 to 50 msec) latch mechanism is electrically deactivated by a signal from the control room or from numerous safety-monitoring systems. When the latch is deactivated it rapidly releases its hold on the air cylinder piston rod and the high pressure air cylinder rapidly drives the control rod(s) to a fully inserted position (maximum permissible scram time is 350 msec). The TREAT reactor is designed to perform transient irradiations for experimental purposes and the reactor is scrammed at the end of each transient (approximately 100 scrams per year).

The rod drive design prior to the upgrade modification had no speed control system to control the impact velocity. The air pressure was set at 300 psi, and a hydraulic dashpot secured to the lower head of the air cylinder was used as a shock absorber. With no speed control, the moving components, which weigh up to 300 lbs, reached impact velocities of 600 in/sec. This peak velocity occured as the cushion plunger entered the hydraulic oil in the dashpot. The shock absorbing forces were produced by increasing oil pressure and fluid friction as the annular clearance between the plunger and the dashpot I.D. became smaller the further the plunger traveled down into the dashpot. A lip seal at the entrance to the dashpot was intended to seal against the cushion plunger and prevent hydraulic fluid from exiting through the air cylinder exhaust port. This seal also redirected the upward movement of oil toward a side-mounted, closed-pipe accumulator.

The dashpot system required considerable maintenance effort to keep it operational. Lip seal life was short due in part to high speed contact with the plunger and to extreme hydraulic conditions as the oil was ejected from the dashpot. Failure of this seal resulted in hydraulic oil expelled from the air cylinder exhaust pipe onto the floor and adjacent rod drives when the reactor was scrammed. The efficiency of the dashpot shock absorbing system was marginal. Recorded rod position during test scrams showed the control rods lifted (or bounced back) 1 inch after contact with the bottom of the dashpot. This "bounce" did not affect the reactor shutdown condition. The poison section of each control rod is 12 inches longer than the core and is centered on the core centerline during shutdown (6 inches above and below the core fuel).

Improvements in the control rod drive scramming systems were successfully completed over a two-year period. This paper will describe the development of an analytical model and the simulations which were critical to the success of the design project. It also describes modifications made to the air cylinder speed control and end cushion portion of the TREAT reactor scramming system improvements.

Computer simulations were performed first, followed by hardware modifications based upon the analytical results, and then full scale testing to simulate reactor operations. An analytical model of a single-cylinder air-drive system with a connecting surge tank was developed which was first used to predict the behavior of the original design. Good agreement between the model and the experimental data was obtained. The model was then modified to describe a design with upper and lower cylinder compartments with surge tanks attached to both. The upper cylinder pressure accelerates the piston initially to provide the insertion of poison and the lower cylinder decelerates it sufficiently to prevent impact damage. Parametric studies were conducted to determine the best combination of upper cylinder upper pressure, surge volume size, and lower cylinder and surge volume size for two different drives--one which must move a heavier weight (two control rods) and another which moves only one control rod. The air drive cylinder was then modified to this optimum design. Data obtained on the new design compared well with analytical predictions.

2. DESCRIPTION OF THE MODEL

The objective of this work was to develop a model which could describe the motion of a control rod when being inserted into a reactor for shutdown. The model is to be used for design studies to redesign the rod insertion mechanism (a piston and cylinder arrangement) so that the rod will be inserted quickly enough and, at the same time, not cause damage to the mechanism when it hits the bottom of the cylinder.

The physical geometry of the problem under consideration is shown in Figure 2. The piston-cylinder arrangement stands vertically. The control rod material is located above the top of the reactor when the piston is in the upper position and is attached to the control rod drive by a non-poison section. The rod is held up by a latch until a scram signal is received. The latch then releases, and the piston is forced down by a pressure differential between the upper side of the piston and the bottom side and by gravity. (The poison is fully inserted in the core when the piston is at the bottom position.) The pressure differential is, by far, the largest of the two forces. A surge tank is connected to the upper cylinder through restricting orifices. This tank and the upper cylinder compartment are pre-pressurized to cause this large force for inserting the rods. A surge tank is also connected to the lower cylinder compartment. Both of these may also be pre-pressurized with the objective of decreasing the piston velocity before it hits the bottom to minimize damage. In addition, a check valve or a bladder may be installed to limit the maximum pressure that can be reached in the lower compartment.

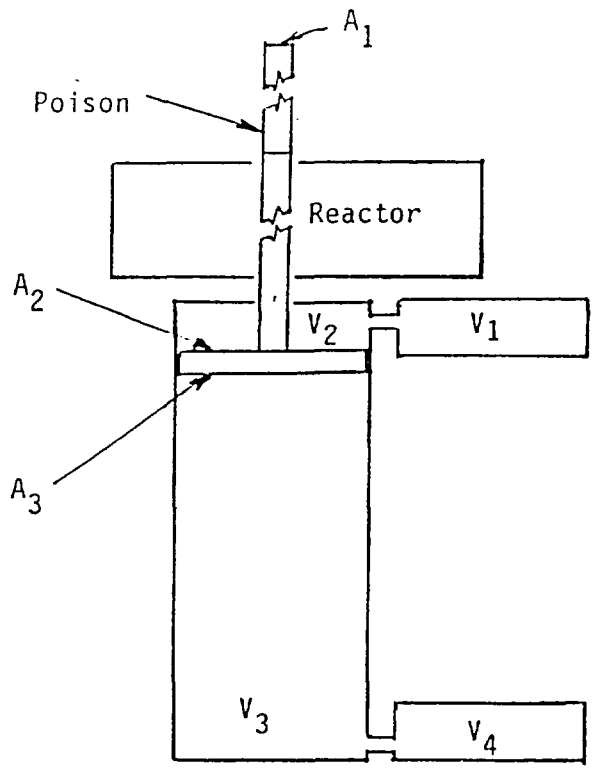

Fig. 2 Schematic of Control Rod Drive Mechanism

A model has been developed which allows the size of the surge volumes, the initial pressures on either side of the piston, and relief valve and bladder settings to be varied. The equations necessary to describe this problem include the equation of motion of the piston, the equations of change for the gas (air) in both compartments of the cylinder and surge tanks, and the equation of motion for the flow between each piston compartment and its respective surge tank.

The energy equations in each of the piston compartments and surge tanks is described by an isentropic equation or, in order to estimate the effect of heat transfer and energy flow due to the flow between compartments, a polytropic equation. The equations for the pressures in volumes 1 and 2 are given by

$$\frac{P_1'}{P_1^0} = \left(\frac{\rho_1'}{\rho_1^0}\right)^n = \left(\frac{m_1'}{V_1'} \cdot \frac{V_1^0}{m_1^0}\right)^n \tag{1}$$

and

$$\frac{P_2'}{P_2^0} = \left(\frac{\rho_2'}{\rho_2^0}\right)^n = \left(\frac{m_2'}{V_2'} \cdot \frac{V_2^0}{m_2^0}\right)^n \tag{2}$$

where $'$ refer to the conditions at a new state and ^{0} refers to conditions at the original state.

The symbols P, rho, m and V refer to the pressure, density, mass, and volume in the respective volumes. The volume in compartment 1 is a constant whereas it varies in volume 2 due to the piston movement.

The equation of motion for flow between compartments is represented by the flow equation for flow through a nozzle with the speed of sound limiting the flow. The equation for the mass flow from the first compartment to the second at any time t through the minimum area A_{12} is

$$\frac{dm_1}{dt} = -\rho_{12} A_{12} v_{12} \tag{3}$$

$$\text{where} \quad \rho_{12} = \rho_1' \left(\frac{P_2'}{P_1'}\right)^{1/k} \tag{4}$$

$$v_{12} = C_{D_{12}} \sqrt{\frac{2g_c k}{k-1} \frac{P_1'}{\rho_1'} \left[1 - \left(\frac{P_2'}{P_1'}\right)^{(k-1)/k}\right]} \tag{5}$$

The flow is restricted by the minimum value of the pressure ratio given as

$$\frac{P_2'}{P_1'} = \left(\frac{2}{k+1}\right)^{k/k-1} \tag{6}$$

which accounts for the critical speed of sound limitation. The mass gain is volume 2 is given by

$$\frac{dm_2}{dt} = -\frac{dm_1}{dt} \tag{7}$$

The above equations represent four independent equations and five unknowns, the pressures and masses in the upper surge tank and upper cylinder, P_1, P_2, m_1, m_2, and the volume of the upper cylinder compartment V_2.

Piston motion is determined with Newton's second law accounting for the pressure forces, gravity, and friction. Atmospheric pressure, P_a, is applied to the portion of the piston represented by the area of the rod, A_1. The equation of motion for the piston is given by

$$m \frac{d^2X}{dt^2} = P_2 A_2 + P_a \cdot A_1 - P_3 \cdot A_3 + mg - F_f \cdot \text{sign} \frac{dX}{dt} \tag{8}$$

where m is the total mass of piston and control rod
X is the position of the piston measured downward
g is the gravitational constant
and F_f is the friction force acting in the direction opposite to the motion.

The value of X solved for from this equation can by related to the volumes

of the upper and lower piston compartments by the following equations:

$$V_2' = V_2^0 + A_2 X \tag{9}$$

and

$$V_3' = V_3^0 - A_3 (L-X) \tag{10}$$

where L is the total length of travel of the piston,
and X=0 corresponds to the top position of the piston.

These three equations have a net effect of introducing one additional unknown, P_3.

The equations of change similar to those of the upper piston compartment and its surge tank and the equation of fluid motion between these compartments but written for the lower piston compartment complete the set of equations so that there are an equal number of equations and unknowns. These equations are obtained by substituting subscripts 3 and 4 for, respectively, 1 and 2 into equations 1 to 7 and specifying that volume 3 varies in size whereas volume 4 remains a constant.

Various boundary conditions can be simulated. Volume 4 can be taken as very large with the initial pressure equal to atmospheric to represent the case where the bottom compartment of the piston is exhausting the atmosphere. A stuck-open relief valve can be simulated by assuming that once a certain pressure is reached, the pressure of volume 4 is equal to atmospheric. A normally operating relief valve can be simulated by specifying that the relief valve is open or closed depending upon the pressure in volume 3. The pressure in volume 4 is either atmospheric or equal to the pressure in a very small volume 4 initialized at the last time of closure. A bladder can be simulated by specifying that the pressure remains a constant in volume 4 once it attains the pressure required for bladder operation.

3. SELECTION OF A SOLUTION METHOD BY STABILITY ANALYSIS

The use of an explicit solution method is desirable because of the speed and simplicity with which it can produce a solution. The stability and, therefore, the possible use of the explicit solution to this non-linear problem is investigated in this section with a subset of the complete equations. The stability of the subset of equations is then investigated by deriving equations which describe the propagation of errors which are introduced by the discretization and truncation numerical errors. These equations are by necessity linearized. Although there is not always a one-to-one correspondence between the stability of linearized equations and those of the original non-linear equations, the agreement is usually close. The objective of the stability analysis is to determine the eigenvalues of the error equations to find out if the errors magnify, diminish, or remain the same.

The subset of equations which describes the flow of a gas from one compartment "a" to compartment "b" through an area "A" is selected for the stability analysis. The approximation for the flow of an incompressible gas is used. The resultant equations in explicit numerical form are given as:

$$m_a(I+1) = m_a(I) - A\sqrt{2\rho_a\left[P_a(I) - P_b(I)\right]}\,\Delta t \tag{1}$$

$$P_a(I+1) = P_a^i\left(\frac{1}{\rho_a^i V_a}\right)^{\gamma} m_a(I+1)^{\gamma} \tag{2}$$

$$m_b(I+1) = m_b(I) + A\sqrt{2\rho_a\left[P_a(I) - P_b(I)\right]}\,\Delta t \tag{3}$$

$$P_b(I+1) = P_b^i\left(\frac{1}{\rho_b^i V_b}\right)^{\gamma} m_b(I+1)^{\gamma} \tag{4}$$

where the variation in the density in the square root is neglected, the flow rate is assumed to be subcritical, and the superscript i refers to the initial condition at time zero.

The stability of this equation set will be investigated by deriving a set of equations which describes the growth of the truncation errors. These are errors which are introduced into the system by using a computer with a finite number of digits. A similar set of equations could also be developed to describe the growth of the discretization error which is due to the necessity of taking a finite instead of an infinitesimal difference increment. Since the second equation set is identical to the first set of error equations, it is only necessary to investigate the stability requirements introduced by the first set. The round-off error may be defined as the difference between the exact solution to the finite difference equations and the numerical solution obtained with a finite number of digits. The former quantities are represented with a circumflex and the latter by a tilda. The error in the mass is then written as

$$E_m \equiv \hat{m} - \tilde{m} \tag{5}$$

The vector of error quantities is then represented by E_j where E_j is defined as

$$E_j = (E_{m_a}, E_{P_a}, E_{m_b}, E_{P_b}) \tag{6}$$

The expressions for the masses and pressures at the new times may be written as non-linear functions of the quantities at the old time. The equation for the round-off error may be obtained by substituting in first the symbol for the exact solution into the equation set given by 1 to 4, second substituting in the symbol for the numerical solution and then subtracting the two equations. When this process is carried out for equation 1, the result is

$$\hat{m}_a(I+1) - \tilde{m}_a(I+1) = \hat{m}_a(I) - \tilde{m}_a(I)$$

$$- \left(A \sqrt{2\rho_a \left(\hat{P}_a(I) - \hat{P}_b(I)\right)} \cdot \Delta t \right.$$

$$\left. - A \sqrt{2\rho_a \left(\tilde{P}_a(I) - \tilde{P}_b(I)\right)} \Delta t \right) \qquad (7)$$

The term on the left hand side of this equation and the first term on the left represents the error in the mass in the "a" volume at the new and the old time. The remaining terms can be put in the form of errors by expanding them in a Taylor's series. Using a Taylor's series approximation for the first term

$$\hat{F} - \tilde{F} = \frac{\partial F}{\partial P_a} \left(\hat{P}_a - \tilde{P}_a \right) + \frac{\partial F}{\partial P_b} \left(\hat{P}_b - \tilde{P}_b \right) \qquad (8)$$

where $F \equiv \sqrt{2\rho_a \left(P_a - P_b\right)}$

$$\frac{\partial F}{\partial P_a} = \frac{1}{2} \cdot \frac{2\rho_a}{\sqrt{2\rho_a \left(P_a - P_b\right)}} = \frac{1}{v} = - \frac{\partial F}{\partial P_b} \qquad (9)$$

and v is the gas velocity between A and B. The partial derivatives are constants evaluated at a suitable reference condition.

Therefore, Equation 7 can be rewritten as

$$E_{m_a}(I+1) = E_{m_a}(I) - \frac{A\Delta t}{v} E_{P_a}(I) + \frac{A\Delta t}{v} E_{P_b}(I) \qquad (10)$$

The equation for the pressure error in volume "a" can be similarly derived from equation 2 as

$$\hat{P}_a\,(I+1) - \tilde{P}_a(I+1) = P_a^i\left(\frac{1}{\rho_a^i V_a}\right)^{\gamma}\left((\hat{m}_a(I+1))^{\gamma} - (\tilde{m}_a(I+1))^{\gamma}\right) \tag{11}$$

Again using a Taylor's series approximation, the equation for E_{P_a} is

$$E_{P_a}(I+1) = P_a^i\left(\frac{1}{\rho_a^i V_a}\right)^{\gamma} \gamma\, m_a^{\gamma-1}\, E_{m_a}(I+1) \tag{12}$$

Substitution of Equation 10 into this equation allows this error to be similarly expressed in terms of errors of quantities at the old time as

$$E_{P_a}(I+1) = k_a\left[E_{m_a}(I) - \frac{A\Delta t}{v} E_{P_a}(I) + \frac{A\Delta t}{v} E_{P_b}(I)\right] \tag{13}$$

where $k_a \equiv P_a^i\left(\frac{1}{\rho_a^i V_a}\right)^{\gamma} \gamma\, m_a^{\gamma-1}$

Similar expressions can be obtained for the other two errors.

The resulting set of equations can be expressed in vector form as

$$\begin{bmatrix} E_{m_a}(I+1) \\ E_{P_a}(I+1) \\ E_{m_b}(I+1) \\ E_{P_b}(I+1) \end{bmatrix} = \begin{bmatrix} 1 & -C & 0 & C \\ k_a & -k_aC & 0 & k_aC \\ 0 & C & 1 & -C \\ 0 & k_bC & k_b & -k_bC \end{bmatrix} \begin{bmatrix} E_{m_a}(I) \\ E_{P_a}(I) \\ E_{m_b}(I) \\ E_{P_b}(I) \end{bmatrix} \tag{14}$$

where $C = \frac{A\Delta t}{v}$

The matrix of these equations determines whether the error is amplified or not. Amplification of the error occurs if one of the eigenvalues is greater than 1. The eigenvalues of this matrix are determined by the solution to the equation

$$D \equiv \begin{vmatrix} 1-\lambda & -C & 0 & C \\ k_a & -k_aC-\lambda & 0 & k_aC \\ 0 & C & 1-\lambda & -C \\ 0 & k_bC & k_b & -k_bC-\lambda \end{vmatrix} = 0 \qquad (15)$$

where this represents a fourth order equation in the eigenvalue lambda. Expansion of this determinant yields the following expression

$$D = (1-\lambda)\lambda^2 \left(-\lambda + (1 - C(k_a+k_b))\right) \qquad (16)$$

Solution of this equation yields

$$\lambda_1, \lambda_2, \lambda_3, \lambda_4 = 1 - C(k_a+k_b),\ 1,\ 0,\ 0 \qquad (17)$$

Thus two of the eigenvalues are always less than one in absolute value. The eigenvalue of one indicates that errors which are introduced will not diminish or amplify. The eigenvalue $1 - C(k_a+k_b)$ can be greater or less than one in absolute magnitude depending upon the time increment chosen. The stability restriction is determined by requiring that

$$-1 \leq 1 - C(k_a+k_b) \leq 1 \qquad (18)$$

The stability requirement comes from the lower limit and requires that

$$\Delta t \leq 2 \frac{|v|}{A} \frac{1}{k_a+k_B} \qquad (19)$$

Since one of the eigenvalues cannot be reduced to a value less than one, and since the actual non-linear equations would be expected to amplify the error more than the linear set considered here, the explicit solution method is expected to be unsatisfactory.

Several calculations were carried out with the equation set 1 to 4 to verify this conclusion. When large pressure drops were investigated, the mass in volume 2 became negative at the second time step. A modification was made to this simple program to describe the motion of the piston. With the pressures in the two volumes set equal at time zero, the solution became unstable immediately due to the perturbation caused by the motion of the piston so the piston motion exacerbates the stability problem with this numerical scheme. Thus the conclusion is reached that the numerical solution of the flow between the two volumes must be obtained with an implicit technique.

4. NUMERICAL SOLUTION METHOD

The method used to solve the equations numerically is described in this section. Initially the procedure involves explicitly solving for the motion of the piston (Equations 8 to 10) to obtain the volumes of V2 and V3. Then the set of equations needed to describe the flow from one volume into another (Equations 1 to 7 of Section 2) is solved implicitly for both the upper and lower cylinder compartments.

The finite difference equations solved for the piston motion are solved first for the piston velocity and then for the position. Equation 8 of Section 2 written in finite difference form for the piston velocity is

$$v_p(I+1) = v_p + (P_2A_2+P_aA_1-P_3A_3 + mg - F_f \text{ sign}\{v\})Dt/m \qquad (1)$$

where all quantities on the right hand side are evaluated at the old time

v_p = piston velocity
Dt = calculational time increment, and
I = time step index

The piston position is then solved for by

$$X(I+1) = X(I) + v_p(I+1)Dt \qquad (2)$$

The volumes of V2 and V3 are solved for from equations 9 and 10 of Section 2 as

$$V_2(I+1) = V_2(I) + A_2DX \qquad (3)$$

where $DX = X(I+1) - X(I)$

$$V_3(I+1) = V_3(I) - A_3DX \qquad (4)$$

Next, the flow of gas from V1 to V2 is solved for implicitly by use of a Newton Raphson iteration technique. An initial estimated value is assigned to the mass in V1 at the new time. Then an estimate of the mass in V2 is made by writing Equation 7 of Section 2 in finite difference form as

$$m_2(I+1) = - m_1(I+1) + (m_1(I) + m_2(I)) \qquad (5)$$

The pressures are solved for from finite difference forms of Equations 1 and 2 of section 2 which are

$$P_2(I+1) = P_2(I)\ \left(\frac{m_2(I+1)}{V_2(I+1)}\ \frac{V_2(I)}{m_2(I)}\right)^n \qquad (6)$$

$$P_1(I+1) = P_1(I)\ \left(\frac{m_1(I+1)}{m_1(I)}\right)^n \qquad (7)$$

Finally, a mass error, F, in volume 1 is solved for from the finite difference form of Equation 3 of Section 2 as

$$F = m_1(I+1) - m_1(I) + \frac{m_1(I+1)}{V_1}\ \left(\frac{P_2(I+1)}{P_1(I+1)}\right)^{1/k}\ A_{12}v_{12} \qquad (8)$$

The gas velocity required in this equation is obtained from Equation 5 of Section 2 with all quantities evaluated at I+1. When F=0, then a solution has been determined at the new time. Two initial estimates are made which bound the solution. The first is the mass at the old time and the second is the mass calculated from Equation 8 with F=0, the pressures equal and the velocity equal to 1200 ft/sec. These two estimates are used to help determine the derivative needed for the Newton Raphson iteration scheme and a new guess of the mass is calculated. The new guess replaces the old guess which is the furthest off and the iteration scheme is continued until a suitably small value of F is obtained. The mass flow is limited by the speed of sound by substituting the pressure ratio specified in Equation 6 whenever the calculated pressure ratio is less than this.

In some cases when the flow resistance is very small, the pressures are very close and a convergent solution is not obtainable with a reasonable number of iterations. In this case, the pressures are set equal and the mass flow rate is solved for by setting the right hand side of Equation 6 to the right hand side of Equation 7 to obtain the equation

$$m_1(I+1) = m_1 + \frac{P_2\ V_{2R}^{1/k} - P_1^{1/k}}{\frac{P_1^{1/k}}{m_1} + \frac{P_2^{1/k}}{m_2}\ V_{2R}} \qquad (9)$$

where all quantities on the right hand side are evaluated at the old time except V_{2R} which is given as

$$V_{2R} = V_2(I)/V_2(I+1)$$

This is the maximum mass transfer rate which can occur for a given change in the volume of V2.

A similar set of equations are solved for the mass transfer from Volume 3 to Volume 4 except that all the subscripts for 1 and 2 are changed to 3 and 4 respectively and due account is taken of the fact that V3 is changing in volume instead of V4.

5. COMPARISON OF COMPUTER MODEL TO EXISTING DESIGN PERFORMANCE

Test data were obtained on the pre-upgrade rod drives in order to provide a basis for checking out the above model. Figure 3 compares the computer model data to recorded control rod position versus time data. Since the testing and computer modeling were completely independent, the accuracy of the model was verified.

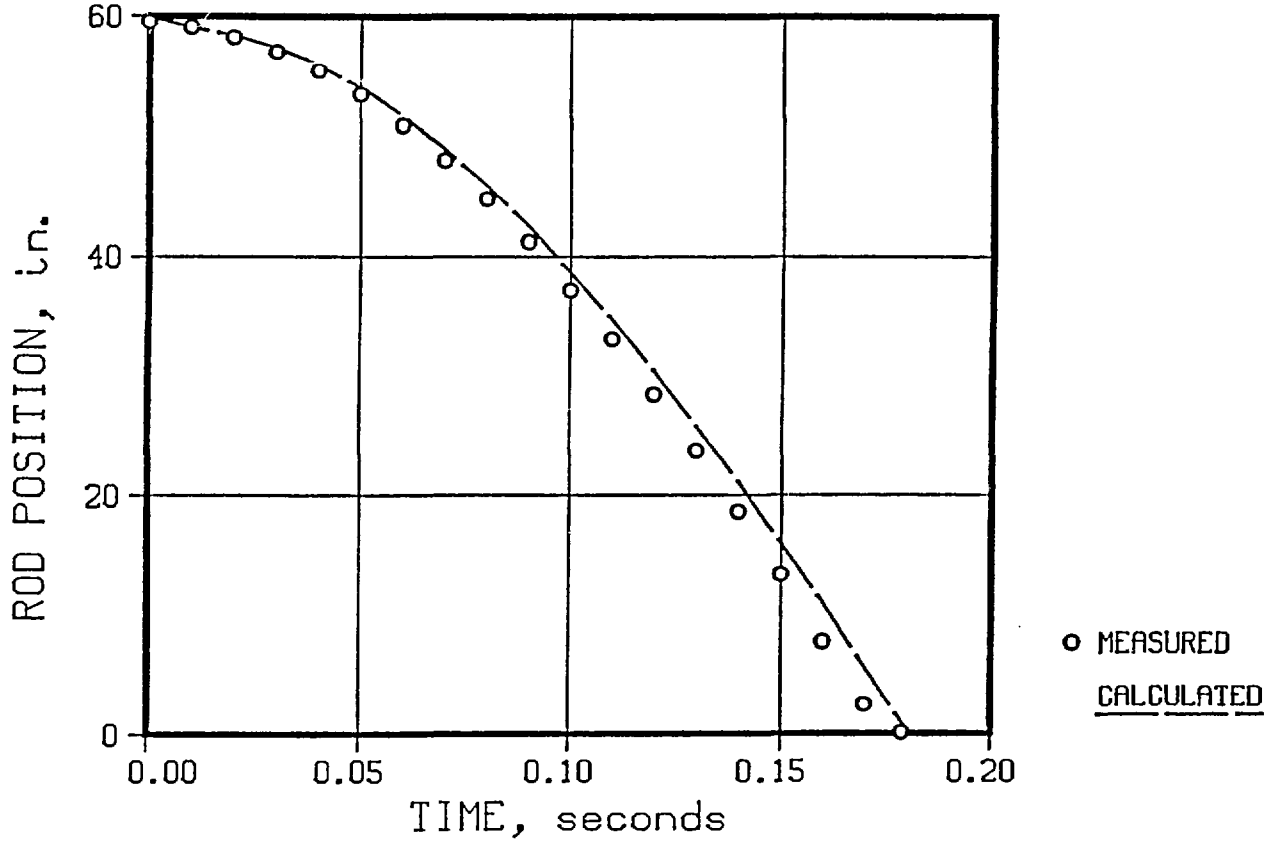

Fig. 3 Rod Position vs Time During Scram

For these tests special instrumentation was added to one of the installed reactor control rod drives. Control rod position, acceleration and deceleration forces were measured during several test scrams from a

full-up initial control rod position. Data were recorded at one msec intervals, and graphs were generated showing rod drive position and accelerometer results versus time. The graphs were used to study rod drive motion during a scram. The control rod velocity could be determined for any elevation during the control rod scram and control rod positions of high "g" loading could be determined. From the data, a peak velocity of 600 in/sec was calculated. This velocity occured as the cushion plunger entered the dashpot. The accelerometer data indicated the major "g" loading occured when the cushion plunger reached the bottom of the dashpot. This transient type shock loading caused a 500 g accelerometer, mounted on one control rod, to produce erratic and apparent over-scale output data. For comparison, the computer model predicted the velocity would be 600 in/sec and that the highest "g" load would be at the end of stroke.

6. DESIGN OF NEW SYSTEM USING ANALYTICAL MODEL

The computer program was designed to allow an input of specific initial conditions i.e.; mass of the moving components, initial piston rod position, supply air pressure, supply air volume, volume of air in the exhaust system, shock absorber data, exhaust air flow restriction data (the original design had minimal restriction of exhaust air flow), were the primary entries. Once the initial conditions were specified the program was run and air cylinder performance data was calculated. As the design progressed the model was modified several times to include additional input and output parameters as needed and the addition of new models to describe new components such as the shock absorber and relief valve which exhausts the air near the end of the piston motion.

Using the qualified program, a trial and error approach was used to determine the end results of changes to the initial conditions. A range of input parameters was investigated to determine a range which sufficiently limited the impact velocity while retaining a short enough scram time. If the initial-supply air pressure was too low and the back pressure on the piston was too high the model would predict a piston bounce (upward movement after or before contact with shock absorber). The model would also calculate how high the piston would bounce with reasonable accuracy (as determined later by testing).

Making small changes in one initial condition at a time and rerunning the program resulted in new information about the air cylinder operation. The original air pressure was found to be higher than desirable. The volume of the built-in supply air surge tank on the rod drive was also too large. Based on results from computer simulations the supply air pressure was reduced from 300 psi to 220 psi and the supply surge tank volume was reduced from 878 in^3 to 272 in^3.

Reducing the drive air pressure and quantity of stored high pressure air available helped to reduce the impact velocity of the piston, but further reduction was still necessary. To reduce further reduce impact velocity into the desired range, the proper size of the lower cylinder

compartment surge tank and inlet orifice were determined. The model showed this method for retarding piston motion near the end of its travel to be adequate. The mechanical design of this method will be discussed later.

The model calculated piston velocity history and the impact velocity from any prescribed release elevation (up to the maximum full out position of 60") to the end of stroke for each revised condition. Running the program for various stroke lengths showed that the peak impact velocity was not at the maximum stroke length (a full-up control rod position) as had been the case for the original design. With the new design the peak velocity occurs when the control rods are scrammed from a 40 inch elevation. This is due to resistance from the air on the exhaust side of the piston available to resist piston movement, and a decrease in the volume of high pressure air on the supply side of the piston. The model

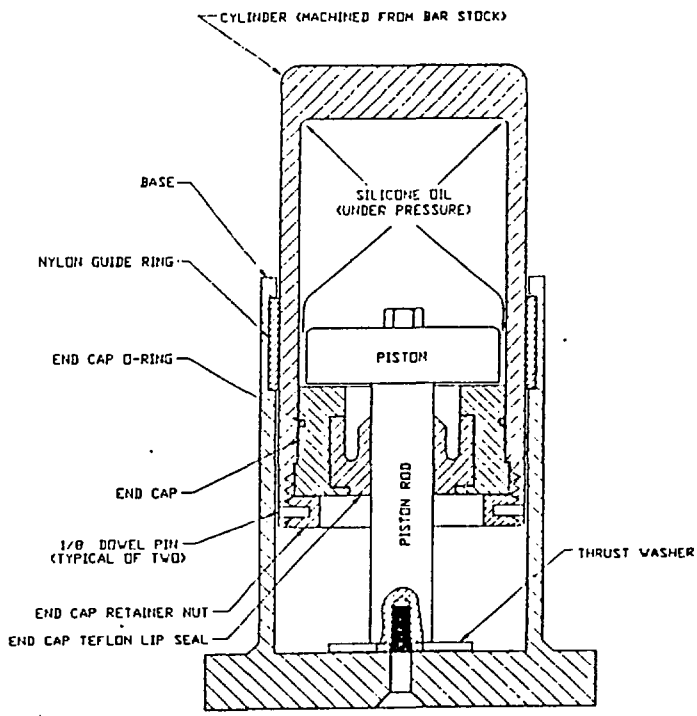

Fig. 4 Compressible Fluid Shock Absorber

predicted an impact velocity range from 100 to 325 in/sec for the new design. Most hydraulic shock absorbers have problems when the impact velocity is either above or below the designed impact velocity. Taylor Devices Inc of North Tonawanda, New York, supplied an acceptable shock absorber. They modified the design of their 2 1/2 inch dia. x 3 inch stroke "Crane Buffer" shock absorber (used in industry for end-stops on overhead bridge cranes) to meet our requirements. This unique shock absorber (see Figure 4) uses a fixed piston, a moving cylinder and a compressible fluid (silicone oil) to provide a square wave shock absorbing

capability. Tests have proven this shock absorber to be extremely forgiving, reliably absorbing shock forces and smoothly stopping motion with impact velocity ranges from 50 to 500 in/sec, and weight variations from 128 to 327 lbs.

The shock absorber cylinder is self extending, eliminating the need for an internal mechanical spring or an external oil accumulator. This feature is due to the compressibility of the liquid. The shock absorber is also sufficiently compact to fit inside a modified dashpot body from the original design rod drive. The dashpot body was center-bored and then counterbored for shock absorber flange attachment through the bottom of the dashpot to allow bottom insertion of the shock absorber (see Figure 5).

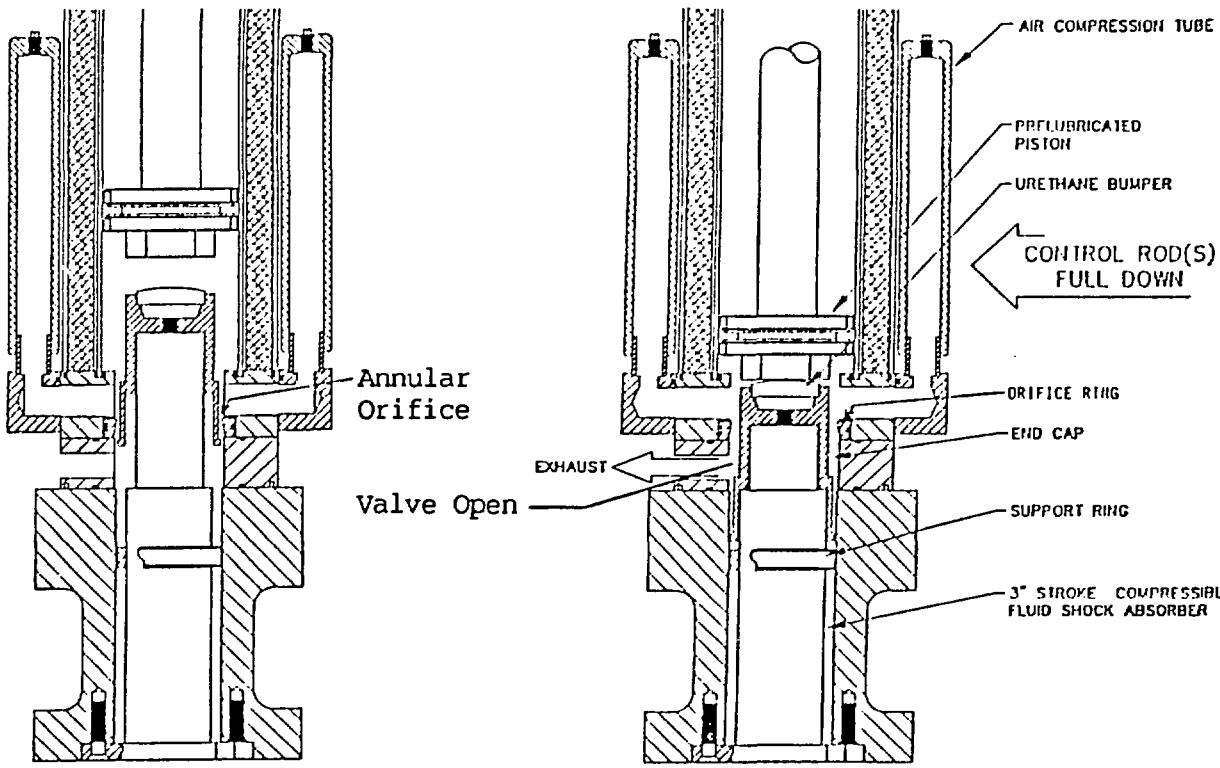

Fig. 5 Refurbished Air Cylinder-Lower Assembly

Once the design of the shock absorber was finalized, the computer model was used to assist in the design of the exhaust air control system. The model was modified to simulate operation of an orifice and a valve to dump the trapped exhaust air unrestricted to atmospheric pressure. It was also modified to include an additional volume (an "air compression tube") connected to the air-cylinder head on the exhaust side of the piston to act as a surge tank. This additional volume was added to control peak deceleration air pressure on the exhaust side of the air-cylinder. The rod position at which the exhaust back-pressure was to be released unrestricted

(like the opening of a relief valve) was also included in the modified model as an input variable. Parametric studies showed that the back-pressure should be released at a rod position of 2 inches from full down to prevent excessive pressure on the decelerating side of the air cylinder piston. At a 2 inch rod position the shock absorber will be compressed 1 inch.

Mechanically, a valve design was implemented by using a stepped-cylindrical end cap for the shock absorber cylinder (see Figure 5). The top of the end cap contains a polyurethane bumper to reduce contact noise when a striker mounted on the air cylinder piston rod end makes contact with the shock absorber end cap. The end cap is partially counterbored to allow its larger diameter end to fit over the top end of the shock absorber cylinder and produce a skirt which extends to a lower elevation than the top end of the shock absorber. The location of the step in the vertical direction was dictated by the location of a sharp edged orifice ring. The orifice ring is installed in an adapter head secured between the lower air cylinder head and the dashpot body (now containing the shock absorber). The outside diameter of the end cap lower half is sized .004 of-an-inch smaller than the orifice ring. The diameter of the upper half of the end cap is 1/2 inch smaller than the orifice ring. Hence, an annular orifice is created between the lower half of the end cap and the orifice ring until the end cap and shock absorber have been moved downward 1 inch. Below the 1 inch point the end cap step permits unrestricted exhaust of the trapped air into a muffler mounted on the outside of the rod drive.

A primary goal of the design project was to reduce the final velocity without appreciably slowing the scram time. Work was also in progress by others in the TREAT group to reduce the time required for the magnetic latch assemblies to release the control rods. This effort resulted in a 40 msec faster release time. Starting rod motion approximately 40 msec faster permitted a 40 msec longer allowable time for rod motion since the scram time is measured from the time the scram signal is initiated until the control rods are full down.

7. DEVELOPMENT AND TESTING OF NEW DESIGNS

a. Control Rod Drive Test Facility

During the above design phase of the reactor upgrade project a test facility was constructed in the TREAT reactor maintenance area to test the computer-assisted control rod drive design. This test facility made use of an existing 3 story experiment assembly structure inside the reactor building high bay. The test location dimensionally simulated an in-reactor rod drive installation. It included a control console which simulated reactor control room controls for rod drive operation and scramming. Mock control rods and control rod guide thimbles were built which modeled the real items. This test facility became an invaluable aid in the final design of the modified rod drives.

b. Testing of Control Rod Drive With 2 Control Rods

The drive which had to move the largest weight (two control rods) was designed first. A control rod drive of the original design was disassembled and modified as described above. After assembly with new and reconditioned parts, the modified rod drive was installed in the test facility where test instrumentation plus upgraded electrical and electronic equipment were installed. High pressure air (up to 300 psi) was made available at the test facility for scramming the new drive. A pressure regulator was added for test purposes. The scram latch power circuit used in the test stand simulated the upgraded reactor latch power circuit.

The prototype rod drive was tested for five months during which all phases of control rod drive operations were tested. Testing of the above end cap design was successful which permitted the performance of other tests in the test stand. The other tests included finding the optimum electrical current setting for the magnetic latch mechanism and the high and low air pressure warning alarm points for in-reactor operation.

The final test for the drive was a series of 300 control rod scramming operations to simulate 3 years of reactor operation. Following this test period the rod drive was dismantled and each component inspected. All components passed the inspection with no signs of abnormal wear.

Test scrams were also performed from every elevation possible and with initial supply air pressure set from 50 psi. to 300 psi. The purpose of the special tests was to observe rod drive performance at abnormal conditions and qualify the new design.

c. Testing of Control Rod Drive With Single Control Rod

Following completion of the above rod drive tests a second control rod drive was designed. The primary differences were the use of only one control rod and the installation of a hydraulic operated latch mechanism. Using the same design with the lighter weight of one control rod would have caused piston bounce. The modification for this rod drive included the same air cylinder changes as described above.

The hydraulic power supply to be used in the upgraded design was installed at the test facility. The hydraulic hose reel and other fittings including control rod guide tubes and a mockup control rod weighing the same as the actual control rod were all installed at the test facility along with the modified control rod drive.

The initial control rod drive test following checkout of the hydraulic latch assembly was the speed control and shock absorber system. The weight of the single control rod moving components was only 128 lbs as compared to the dual control rod magnetic latch moving components of 273 lbs. The result of the lighter weight was an increase in impact velocity on the

shock absorber. The momentum of the single rod system, however, was approximately 1/3 less than the momentum of the dual rod system. The shock absorber brought both moving systems safely to rest with reserve capacity. The only difference between the two air cylinder speed control systems is the volume of the exhaust surge tanks. Because the momentum of the single rod system is less, the surge tank volume had to be increased to keep the minimum scram air pressures identical for the two systems. The surge tank volume for the single rod system is 1/3 larger than the surge tank volume for the dual rod system. This change permitted the low air pressure scram switch settings to be at the same air pressure for both rod drive systems. The volume available for air compression on the exhaust side of the piston directly affects the minimum acceptable supply air pressure. The larger the volume the lower the pressure requirement.

8. COMPARISON OF NEW DESIGN TO PREDICTIONS AND TO ORIGINAL DESIGN

The test facility allowed a check of rod drive performance against computer predictions and against performance by the pre-upgrade design rod drive. Data during the above tests were recorded by computer for most scrams performed. Rod position and upper and lower cylinder compartment air pressures were recorded versus time. A typical result for the dual rod drive is shown in Figure 6. The upper cylinder pressure decreases throughout the insertion. The lower cylinder air pressure is seen to increase as the piston moves down until the end-cap valve opens allowing the trapped air to escape.

The rod position versus time is similar to that of Figure 3 for the unmodified rod drive. The core is effectively shut down by the time the rods are inserted half way and both designs reach this position within about 1 msec of each other. Full insertion occurs about 5 msec later in the new design than the original design because of the desired reduction in the impact velocity. The impact velocity is 330 in/sec for the new design compared with 600 in/sec for the original design.

Predicted values for position and pressures versus time are also included in Figure 6. The behavior in the calculation and measured values is seen to be similar. The impact velocities, rod position, and air compression pressures (except peak pressure) predicted by the computer for the dual rod design are within 10 percent of measured values. The largest discrepancy measured was the peak air compression pressures which occurs near the end of the piston travel. This is very difficult to predict because a small error in the calculated volume near the end of the stroke will make a large error in the pressure. The code calculated the momentary peak pressure to be approximately thirty percent greater than that measured. This discrepancy may have resulted more from a pressure transducer response too slow to measure the transient type pressures encountered. The location of the step in the end-cap and the size of step needed was accurately predicted by the code and no changes were required.

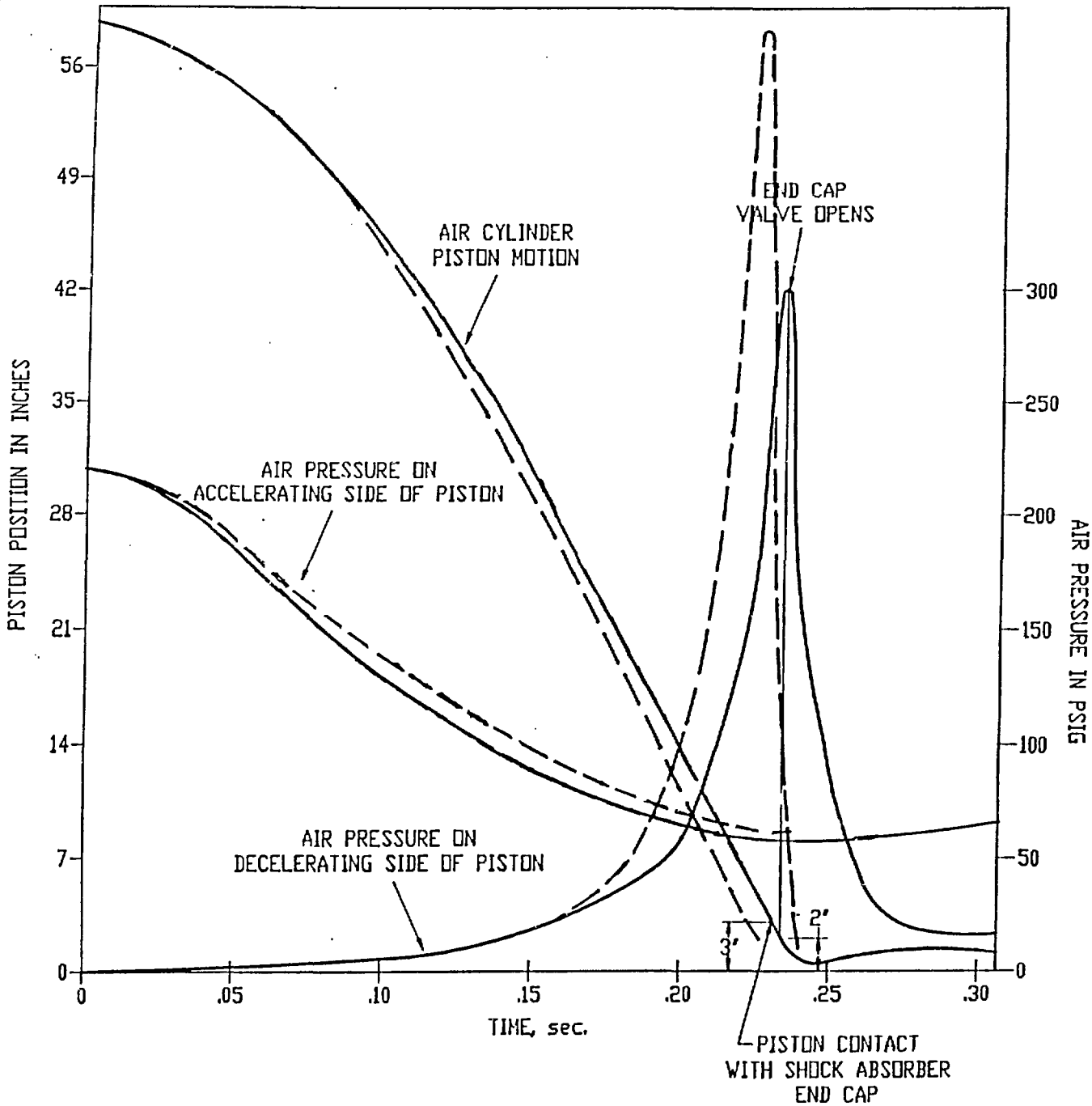

Fig. 6 Behavior of Modified Control Rod Drive

9. CONCLUSIONS

When the original control rod drives were in their design stage 30 years ago the plan was to provide a separate hydraulic shock absorber end cushion along the same lines as the upgrade design. That initial project did not meet its objective—not because it was a bad idea, but the design engineers did not have the computer model advantage. They did build a test facility which proved the initial design to be faulty. A second generation rod drive design using the hydraulic dashpot discussed early in this paper was later developed and tested. This second rod drive design was used until the end of 1987.

No attempt at speed control was made for either of the above designs and materials like polyurethane for the end-cap striker surface plus the compressible fluid shock absorber were not available for their use. Hence, the idea was there in 1958 but the simulation techniques and advanced materials were not.

The key to the success of the upgraded TREAT reactor control rod drive modifications was the computer simulation code which permitted design flexibility and accurately predicted the results of proposed design changes. It provided a cause and effect design effort so the design failures could be weeded out before the product was built. The test stand facility was very important but before it could be adequately utilized the design needed refinements only possible through computer simulation. The shock absorber, for example, could not have been designed properly without the air cylinder performance information the code provided.

In summary, operation of the rod drives in a test stand which accurately simulated installed reactor conditions provided a quality end product. The tests demonstrated the validity of the computer simulation code as well as the reliability of the modified control rod drive design. The design goals were achieved. The final result is a control rod drive design which minimizes maintenance efforts and exceeds design requirements. This was made possible through the use of computer simulation design aids and "state-of-the-art" engineering materials.

Authors' Footnote

The TREAT control rod drive upgrade provided a very unique opportunity for both the design engineer and the author of the computer model. We were able to follow the design of the system from computer simulation through testing, installation, and successful operation in the reactor.

Acknowledgement This work was sponsored by the U.S. Department of Energy, Office of Nuclear Energy, Facilities, Fuel Cycle, and Test Programs, under contract W-31-109-ENG-38.